

# EFFECTS OF CONFINEMENT ON A TWO-DIMENSIONAL SYSTEM OF THE LENNARD-JONES PARTICLES IN SPHERICAL GEOMETRY\*

PAWEŁ KARBOWNICZEK, AGNIESZKA CHRZANOWSKA

Institute of Physics, Cracow University of Technology  
Podchorążych 1, 30-084 Kraków, Poland

(Received May 29, 2013)

Influence of confinement on a two-dimensional Lennard-Jones system of spherical particles has been studied by means of Molecular Dynamics simulations. High Resolution Density Map (HRDM) method has been applied to study of inhomogeneous configurations in a circular geometry. Solidification has been shown to depend strongly as well on the structure as on the type of constituting particles of the surrounding wall. Within the liquid state, for certain parameters of density and temperature, configurations occur that remind of the structure of node lines characteristic for the Bessel equation, which are argued to play the role of the seeds for solidification.

DOI:10.5506/APhysPolB.44.1209

PACS numbers: 61.20.-p, 64.70.dm, 61.20.Ja

## 1. Introduction

Study of the structure of fluids and their mixtures in confined geometries is an interesting area of research because of its relevance to surface driven phase transitions, adsorption, wetting *etc.* [1]. Hence, it arises a strong interest in the field of theoretical and computer simulation studies of fluids in pores, slits and other geometries. Confined fluids behave very differently in comparison to the bulk fluids. Interesting aspects of the confinement include non-uniform density distributions [2], adsorption hysteresis effects [3], preferential adsorption in mixtures [4], effects at the solid–liquid interface [5] and phase transitions [6]. Inhomogeneous behavior is often caused by the fluid–solid interactions, competition between fluid–solid and fluid–fluid forces and

---

\* Presented at the XXV Marian Smoluchowski Symposium on Statistical Physics, “Fluctuation Relations in Nonequilibrium Regime”, Kraków, Poland, September 10–13, 2012.

the excluded volume effect [7–9]. Fluids confined in small nanoscale pores are common in nature. Typical examples of porous materials include carbon nanotubes, activated carbon, silica gel and zeolites [10].

Using Molecular Dynamics, Monte Carlo and Density Functional Theory confined fluids have been widely investigated according to the literature (see [8] and references therein). At the molecular level, inhomogeneous fluids are frequently studied using a slit pore geometry, which consists of two parallel walls (see for example [9] or [11]). This model allows to change the degree of confinement in a convenient way. For the confined fluid, a decrease in the confined scale leads to a larger portion of fluid molecules interacting with the wall. Real porous materials, however, show a more complex structure made of interconnected network of pores. In recent years, the physics of phase transitions in lower-dimensional systems has attracted interest with emphasis on the two-dimensional liquid to solid transition [8, 12]. It is known that freezing and melting behavior of confined fluids may deviate strongly from bulk behavior [13]. Confinement induces layering at the walls in the liquid phase and, therefore, has significant influence on the process of crystallization. The crystallization process changes significantly, depending on the strength of the particle-wall interaction [14]. In the case of strongly attractive walls, crystallization starts from the walls at a temperature higher than the transition temperature in the bulk system. In the opposite situation, when the walls are strongly repulsive, crystallization starts from the bulk at a temperature lower than the temperature of the system without introduced confinement. Studies of slit pores show that the shift in crystallization temperature is dependent on the nature of the walls [15]. In a two-dimensional case, the crystallization of a layer of the Lennard-Jones particles [16] is, however, expected to proceed through the KTHNY mechanism [17], which differs from the bulk nucleation. The phase diagram of fluids confined in porous materials can be, therefore, different than those observed in bulk due to the geometrical constraints.

The simple structureless models of the wall-fluid interactions like the Steele, 9–3 (where 12 and 6 coefficients in the Lennard-Jones potential are replaced by 9 and 3, respectively) and 10–4 potentials are often used in simulations. The Steele 10–4–3 potential [18] is given by

$$U_{\text{wf}}(x) = 2\pi\rho_S\sigma_{\text{wf}}^2\epsilon_{\text{wf}} \left[ \frac{2}{5} \left( \frac{\sigma_{\text{wf}}}{x} \right)^{10} - \left( \frac{\sigma_{\text{wf}}}{x} \right)^4 - \frac{\sigma_{\text{wf}}^4}{3\Delta(x + \alpha\Delta)^3} \right], \quad (1)$$

where  $x$  is the distance between the fluid particle and the wall,  $\Delta$  interlayer spacing of the wall atoms,  $\rho_S$  is the carbon density on the slab surface,  $\sigma_{\text{wf}}$  and  $\epsilon_{\text{wf}}$  are the wall-fluid interaction parameters and  $\alpha = 0.61$  is an empirical adjustment improving accuracy of the model of a pore wall. The first two terms of the potential comes from the first plane of the wall interacting

via the Lennard-Jones potential with the inner system, whereas the third comes from the other layers infinitely extended down from  $\alpha$  with  $\rho_S$  density. Despite the fact that these potentials became the most popular in the literature, they are simplified and do not take into account structure of the wall, therefore they cannot describe all the physical processes that might occur in porous materials.

## 2. Application of HRDM method to the confined systems

A 2D system of the spherical Lennard-Jones particles is considered in the spherical confinement. For this purpose, an appropriate Molecular Dynamics program, which allows for simulations at different thermodynamic conditions and for different potential parameters, has been written. All calculations are performed in reduced units, where time corresponds to the actual time of several ps (depending on the type of the particles). Note, however, that this range of time is still unattainable in the real experiments. The Lennard-Jones particles in the considered confined geometry are composed of inner particles of one type and particles constituting the edge of the closed geometry (as in Fig. 1). This case is similar to a binary mixture, although the positions of the wall particles are fixed. Compared to the unrestricted particle system, the external potential originating from the wall causes the complex structures in the density distribution near the walls. Fully atomistic representation used in this publication reproduces behavior at the wall-fluid interface better than integrated potentials like 10–4 or Steele 10–4–3.

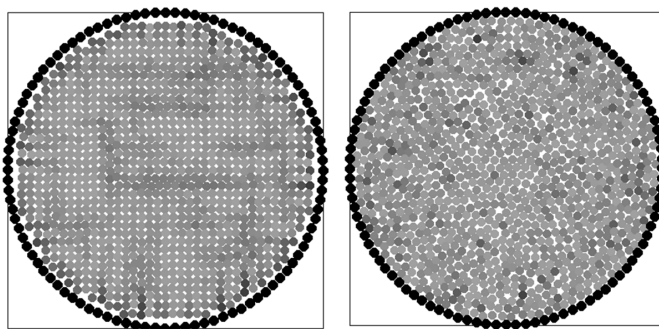


Fig. 1. Sample configurations of the simulated system. The left panel shows a square lattice and the right configuration after equilibration of the system. Different shades of gray represent different kinetic energy of the particles — the darker they are the more kinetic energy they have.

Let us consider the two-dimensional space, in which a point is given by

$$\mathbf{z} = (z_x, z_y) \in \mathbb{R}^2. \quad (2)$$

The particles inside the container interact among themselves via the Lennard-Jones potential

$$U_{11}(r) = 4\epsilon_{11} \left[ \left( \frac{\sigma_{11}}{r} \right)^{12} - \left( \frac{\sigma_{11}}{r} \right)^6 \right], \quad (3)$$

where  $\epsilon_{11}$  is the depth of the potential well,  $\sigma_{11}$  is the distance at which the inter-particle potential is zero;  $r$  is the inter-atomic distance. For simulation purposes, potential was truncated and shifted in the cutoff radius  $r_c = 2.5\sigma_{11}$ . System particles can also interact with the wall, which is built from the spheres, whose size and potential well can be modulated. The edge is constructed by placing the particles of the chosen size in such a manner that they form a closed circle with unitary linear density. Then the system particles are placed inside this ring. We assume that the edge particles are immobile relative to each other. The  $N$  particles confined inside the structured geometry interact with  $M$  edge geometry particles via the Lennard-Jones potential

$$U_{12}(r) = 4\epsilon_{12} \left[ \left( \frac{\sigma_{12}}{r} \right)^{12} - \left( \frac{\sigma_{12}}{r} \right)^6 \right], \quad (4)$$

where  $\epsilon_{12}$  and  $\sigma_{12}$  are the wall-fluid interaction parameters. Since in reality any edge or the wall influences the system molecules that find themselves in its vicinity, we assume here also an appropriate interaction for this influence. The effective parameters fulfill the Lorentz–Berthelot mixing rules [19]

$$\epsilon_{12} = \sqrt{\epsilon_{11}\epsilon_{22}} \quad (5)$$

and

$$\sigma_{12} = \frac{\sigma_{11} + \sigma_{22}}{2}, \quad (6)$$

respectively. In the above equation,  $\epsilon_{22}$  and  $\sigma_{22}$  are the parameters of the potential of the edge geometry particles. The potential field originating from the geometry will be given then as a sum of all the potentials from all molecules constituting the edge. Let us take, for example, a circle built from  $M$  particles, whose radius is equal to  $Z$ . The effective potential field, taking into account the Lorentz–Berthelot coefficients, will be given as

$$U_{\text{field}}(\mathbf{z}) = \sum_{i=1}^M U_{12}(\mathbf{z} - \mathbf{z}_i), \quad (7)$$

where  $\mathbf{z}_i = (Z \cos(2\pi i/M), Z \sin(2\pi i/M))$  are the positions of the edge particles distant by  $Z$  from the center of the geometry. The system particles, which are being placed inside the circular area of the radius  $Z$ , will be affected then by the above potential. In a similar way, one can build other geometries.

In Fig. 2, sample potential field that comes from the particles constituting the wall is presented. This effective potential is assumed as a simple sum of the contributions from all the wall particles. As a consequence, the state of the particles system inside a pore will be determined by two factors: by the thermodynamic parameters as in the bulk systems and by the details of confinement. In practice, the simulation is performed as follows. First, a starting configuration is prepared and its size is adjusted to the pore geometry, then the actual Molecular Dynamics is performed. The starting configuration can be taken either from the equilibrated bulk system, or created “by hand” like, for instance, square lattice in Fig. 1, where the equilibration process drives the system into the hexagonal arrangement via non-equilibrium restructuring process manifested in linear and cross structures in the distribution of the kinetic energy [20].

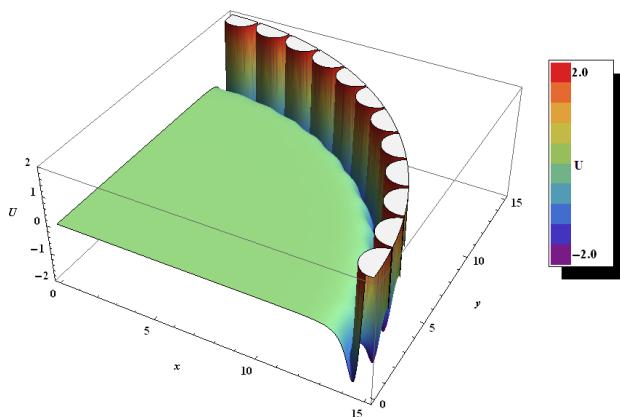


Fig. 2. Sample potential field resulting from the edge geometry.

In principle, the HRDM method is destined to study features of the structured media, therefore, it is inappropriate for liquid state. However, the existence of the cohesive walls causes to occur layers at the walls, the number of which and their structure depends on the thermodynamic parameters. The closer system is to the transition to the solid phase the more pronounced these features are. In order to study features around the liquid–solid transition point, a sequence of initial configurations has been prepared by the use of the bulk system program. From the equilibrated configurations for a chosen temperature and density, for a given point from the bulk

phase diagram, we cut out a spherical sample that would fit to the assumed container. Different graphical filters and color palettes have been applied to enhance the picture details. The first effect that should be noted at the beginning is that one cannot preserve the same number of the density. As seen in the left panel of Fig. 1, there is a little free space near the wall, so effectively we will deal with a slightly smaller density. Such prepared samples are then equilibrated, so the particles could attain their more preferable states. To get the more interesting results, where the HRDM method can be used, the thermodynamic points (particular values of the temperature and density) at which the simulation must run are taken from the bulk phase diagram in the vicinity of the transition line between liquid and solid. In fact, one expects here that confinement will change the position of this line. There is also another problem worth noting: whether the notion of a solid is applicable and in what sense in the case of small systems. Can we still use a word “solid” in the case of several or even tens or hundreds of particles?

In the present work, the particles in the confinement are described by different parameters. NVE simulations were performed for initial densities of 0.8, 0.95 and 1.0 and final temperatures around 1. Results are presented in Fig. 3 for three different densities, three different size ratios between the inner system and the wall particles  $\sigma_{11}/\sigma_{22}$ , identical potential well depths  $\epsilon_{11} = \epsilon_{22} = 1.0$ , radius of the geometry equal 20 distances at which the Lennard-Jones potential of the inner system particles reaches its minimum and time of the simulation after initial equilibration equal 1000.0 with the time step  $\Delta t = 0.002$ . Wall particles were placed with linear density equal to 1.0. For the density equal to 0.8, the system is still in a liquid state, but at the walls one can observe a structure that depends on the type of the wall. For the wall particles twice larger than the system particles, this structure consists of well localized and less mobile particles — there is a visible ring of dark and lighter spots. Decreasing the size of the wall particles results in the effective potential at the wall, which no longer consists of the well separated wells, but reminds of a crevice within which the system particles can freely change their position. As a result, one observes two well distinguished light rings and another two slightly less visible rings. Upon increasing density the system shifts its state toward the solid. However, new features can be observed depending as well on the density as on the wall particle sizes. The most striking feature is what we call here the Bessel like structure. By comparing these pictures with the solutions of the circular membrane Bessel equation (which is just the condition for vanishing the Laplacian), we find the similarity for the case of the sixfold radial lines of nodes. In principle, there are many different particular solutions to the membrane equation together with the type of node lines. Taking into account that the hexagonal symmetry is the most preferable configuration symmetry for

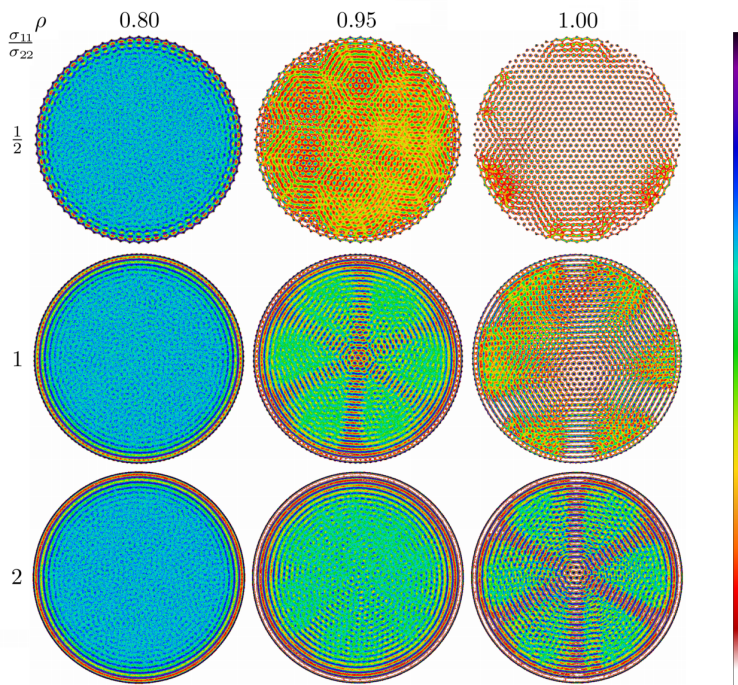


Fig. 3. Sample High Resolution Density Maps of the Lennard-Jones system confined in a circle geometry. Gradient from the side is a density scale ranging from 0 (white) to the maximum value (black).

an unlimited two-dimensional case, it may come as natural that sixfold line realizes here. Note that the basic determining factor, in the case of circular membrane, is the shape of the boundary. The observed structure might be the effect of the diffusional equation for the density, but this hypothesis still requires more consideration. The existence of the node lines has its straightforward consequences — they can be immediately regarded as the seed areas for the crystallization process. This effect is a new outcome for the small and confined systems. In fact, it is not clear whether such effect will be present in larger systems. On the one hand, the node lines are the general outcome, but on the other hand, the influence of the walls on the system becomes smaller upon increasing size of the system. Looking at the map, one observes an immobile hexagonal domain in the middle of the sample which definitely grows upon increasing the density. This is a new feature, since so far the crystallization process in the presence of the cohesive wall was regarded as starting from the wall layers. Looking at the panels in the rows showing the maps of the system for different sizes of the wall particles, it is also visible that diminishing the size of the walls particles

shifts the crystallization process toward higher densities. Thus, another conclusion here is also that the more structured walls enhance the process of crystallization. In Fig. 4, the Fourier transforms corresponding to the density maps from Fig. 3 are presented. It is interesting to see how the new features described above manifest themselves in the FFT presentation. The 2nd, 3rd, 6th and 9th panels give evidence about more established hexagonal order. One can also conclude that occurrence of six short stripes situated on the rings in the FFT images is associated with the six radial node lines in the real configurations.

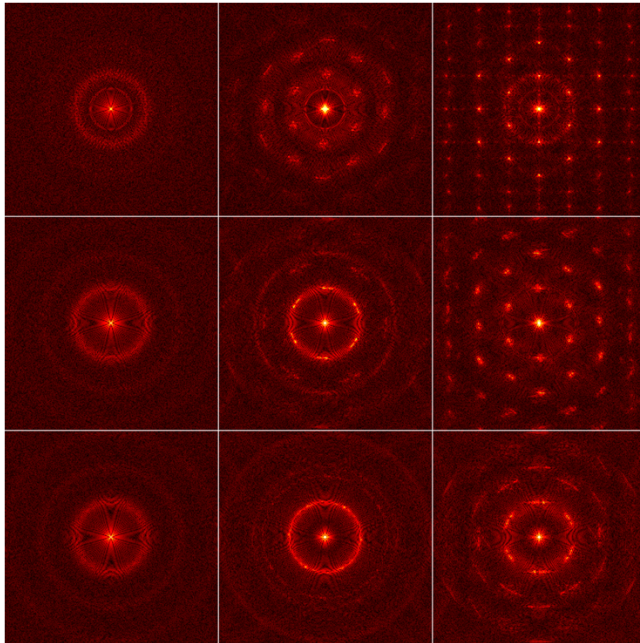


Fig. 4. Fast Fourier Transforms for the High Resolution Density Maps from the previous figure.

### 3. Summary

In the present work, we show High Resolution Density Maps obtained from Molecular Dynamics simulations of the small systems of the particles confined to the pore of a circular shape for the densities for which the system is close to the liquid–solid transitions. The most striking observation is the occurrence of the node density lines like in the Bessel problem, which play the role of the seed areas for solidification.

## REFERENCES

- [1] C.A. Croxton, *Fluid Interfacial Phenomena*, Wiley, New York 1986; C. Domb, J.L. Lebowitz, *Phase Transition and Critical Phenomena*, Academic Press, New York 1988; J. Toth, *Adsorption: Theory, Modeling, and Analysis*, Dekker, New York 2002.
- [2] J.J. Magda, M. Tirrell, H.T. Davis, *J. Chem. Phys.* **83**, 1888 (1985); B.K. Peterson *et al.*, *J. Chem. Phys.* **88**, 6487 (1988).
- [3] G.S. Heffelfinger, F. van Swol, K.E. Gubbins, *J. Chem. Phys.* **89**, 5202 (1988).
- [4] C. Gu *et al.*, *Fluid Phase Equilibria* **194–197**, 297 (2002).
- [5] F.F. Abraham, *J. Chem. Phys.* **68**, 3713 (1978).
- [6] G.S. Heffelfinger, F. van Swol, K.E. Gubbins, *Mol. Phys.* **61**, 1381 (1987); J. Klein, E. Kumacheva, *J. Chem. Phys.* **108**, 6996 (1998); Y.C. Yortsos, A.K. Stubos, *Curr. Opin. Colloid Interface Sci.* **6**, 208 (2001).
- [7] D. Henderson, *Fundamentals of Inhomogeneous Fluids*, Dekker, New York 1992.
- [8] L.D. Gelb, K.E. Gubbins, R. Radhakrishnan, M. Sliwinska-Bartkowiak, *Rep. Prog. Phys.* **62**, 1573 (1999).
- [9] T.K. Vanderlick, L.E. Scriven, H.T. Davis, *J. Chem. Phys.* **90**, 2422 (1989).
- [10] A.E. Scheidegger, *The Physics of Flow Through Porous Media*, Macmillan, New York 1957; M. Śliwińska-Bartkowiak *et al.*, *Phys. Chem. Chem. Phys.* **3**, 1179 (2001).
- [11] N. Gribova *et al.*, arXiv:0902.3344 [cond-mat.soft].
- [12] K.J. Strandburg, *Bond-Orientational Order in Condensed Matter Systems*, Springer-Verlag, New York 1992.
- [13] R. Evans, *J. Phys.: Condens. Matter* **2**, 8989 (1990).
- [14] C. Alba-Simionesco *et al.*, *J. Phys.: Condens. Matter* **18**, R15 (2006).
- [15] M. Miyahara, K.E. Gubbins, *J. Chem. Phys.* **106**, 2865 (1997); H. Dominguez, M.P. Allen, R. Evans, *Mol. Phys.* **96**, 209 (1999).
- [16] J.E. Lennard-Jones, *Proc. R. Soc. Lond. A* **106**, 463 (1924).
- [17] J.M. Kosterlitz, D.J. Thouless, *J. Phys.* **C5**, L124 (1972); *J. Phys.* **C6**, 1181 (1973); J.M. Kosterlitz, *J. Phys.* **C7**, 1046 (1974); D.R. Nelson, J.M. Kosterlitz, *Phys. Rev. Lett.* **39**, 1201 (1977); B.I. Halperin, D.R. Nelson, *Phys. Rev. Lett.* **41**, 121 (1978); D.R. Nelson, B.I. Halperin, *Phys. Rev.* **B19**, 2457 (1979); A.P. Young, *Phys. Rev.* **B19**, 1855 (1979).
- [18] W.A. Steele, *Surf. Sci.* **36**, 317 (1973).
- [19] J.S. Rowlinson, *Liquids and Liquid Mixtures*, Butterworth Scientific, London 1982.
- [20] P. Karbowiczek, A. Chrzanowska, *J. Chem. Phys.* **134**, 044527 (2011).